

Strong excitation intensity dependence of the photoluminescence line shape in GaAs_{1-x}Bi_x single quantum well samples

Yu. I. Mazur, V. G. Dorogan, M. Schmidbauer, G. G. Tarasov, S. R. Johnson, X. Lu, M. E. Ware, S.-Q. Yu, T. Tiedje, and G. J. Salamo

Citation: *Journal of Applied Physics* **113**, 144308 (2013); doi: 10.1063/1.4801429

View online: <http://dx.doi.org/10.1063/1.4801429>

View Table of Contents: <http://scitation.aip.org/content/aip/journal/jap/113/14?ver=pdfcov>

Published by the AIP Publishing

Articles you may be interested in

[Insight into the epitaxial growth of high optical quality GaAs_{1-x}Bi_x](#)

J. Appl. Phys. **118**, 235701 (2015); 10.1063/1.4937574

[Low temperature magneto-photoluminescence of GaAsBi /GaAs quantum well heterostructures](#)

J. Appl. Phys. **115**, 123518 (2014); 10.1063/1.4869803

[Temperature dependent photorefectance and photoluminescence characterization of GaInNAs/GaAs single quantum well structures](#)

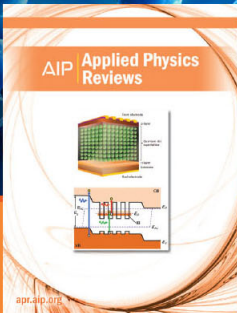
J. Appl. Phys. **96**, 6298 (2004); 10.1063/1.1805724

[Photoluminescence and photorefectance study of InGaAs/AlAsSb quantum wells grown by molecular-beam epitaxy](#)

J. Appl. Phys. **95**, 1050 (2004); 10.1063/1.1637936

[Optical properties of InGaAs/AlAsSb type I single quantum wells lattice matched to InP](#)

J. Vac. Sci. Technol. B **19**, 1747 (2001); 10.1116/1.1394727



NEW Special Topic Sections

NOW ONLINE
Lithium Niobate Properties and Applications:
Reviews of Emerging Trends

AIP | Applied Physics Reviews

Strong excitation intensity dependence of the photoluminescence line shape in GaAs_{1-x}Bi_x single quantum well samples

Yu. I. Mazur,^{1,a)} V. G. Dorogan,¹ M. Schmidbauer,² G. G. Tarasov,³ S. R. Johnson,⁴ X. Lu,⁴ M. E. Ware,¹ S.-Q. Yu,⁵ T. Tiedje,⁶ and G. J. Salamo¹

¹Department of Physics, University of Arkansas, 226 Physics Building, Fayetteville, Arkansas 72701, USA

²Leibniz-Institute for Crystal Growth, Max-Born-Str. 2, D-12489 Berlin, Germany

³Institute of Semiconductor Physics, National Academy of Sciences, pr. Nauki 45, Kiev 03028, Ukraine

⁴Department of Electrical Engineering, Arizona State University, Tempe, Arizona 85287-6206, USA

⁵Department of Electrical Engineering, University of Arkansas, 3217 Bell Engineering, Fayetteville, Arkansas 72701, USA

⁶Department of Electrical and Computer Engineering, University of Victoria, Victoria, British Columbia V8W 3P6, Canada

(Received 18 March 2013; accepted 27 March 2013; published online 10 April 2013)

A set of high quality single quantum well samples of GaAs_{1-x}Bi_x with bismuth concentrations not exceeding 6% and well widths ranging from 7.5 to 13 nm grown by molecular beam epitaxy on a GaAs substrate at low temperature is studied by means of photoluminescence (PL). It is shown that the PL line shape changes when the exciton reduced mass behavior changes from an anomalous increase ($x < 5\%$) to a conventional decrease ($x > 5\%$). Strongly non-monotonous PL bandwidth dependence on the excitation intensity is revealed and interpreted in terms of optically unresolved contributions from the saturable emission of bound free excitons. © 2013 AIP Publishing LLC. [<http://dx.doi.org/10.1063/1.4801429>]

I. INTRODUCTION

The physical properties of dilute GaAs_{1-x}Bi_x/GaAs heterostructures are in the focus of recent investigations due to their potential in the development of various opto-electronic devices for the mid-infrared spectral region.¹⁻³ It has been shown that a small quantity of Bi added to host GaAs material quickly reduces the band gap with a rate of ~ 90 meV/% of Bi.¹ This reduction, however, is not observed symmetrically at the conduction and valence band edges. Nearly all of the shift appears in the valence band maximum while the conduction band minimum moves only slightly. A significant advancement in the study of the GaAsBi material system has been made possible through the development of controllable molecular beam epitaxial growth of GaAs_{1-x}Bi_x layers on GaAs in the form of single quantum well (QW) and multiple QW structures which demonstrate good structural quality and strong photoluminescence (PL) emission without the necessity of annealing.^{3,4} Recently, many questions have been explored concerning the origin of the Bi induced reduction of the band gap, character of impurity distribution, and the mechanisms of effective PL emission in order to provide a clear understanding of GaAs_{1-x}Bi_x/GaAs physics. For example, it has been established that GaAsBi alloys demonstrate clustering, phase separation, and atomic ordering depending on the Bi concentration range.⁵⁻¹² These effects can significantly influence the optical and electrical properties of GaAs_{1-x}Bi_x/GaAs heterostructures.¹³⁻¹⁵

Most current research on GaAs_{1-x}Bi_x/GaAs heterostructures is concerning comparatively thick epilayers, ~ 30 – 40 nm;¹⁰⁻¹² however, unique features arise in the optical studies of thin GaAs_{1-x}Bi_x layers due to spatial confinement.¹⁶

We have reported the results of a PL study of a 11 nm GaAs_{0.94}Bi_{0.06} film embedded in GaAs and grown by molecular beam epitaxy (MBE) at low temperature. The low temperature PL of this material exhibited a pronounced blue-shift as both temperature and excitation intensity increased which was attributed to the defect controlled radiative recombination of localized excitons and the evolution of excited states with a QW. Although carrier localization in GaAsBi epilayers has been discussed previously,^{2,17,18} a detailed description of the excitation-intensity dependent PL is still required to completely understand the nature of the carrier dynamics in regions of concentration fluctuations including clustering of Bi atoms. In the present work, the excitation intensity dependence of PL is studied for a set of GaAs_{1-x}Bi_x single QWs at 15 K in order to specify the carrier localization mechanisms.

II. EXPERIMENTAL RESULTS AND DISCUSSIONS

We present here the results for three MBE-grown GaAs_{1-x}Bi_x QWs. These samples are basically those described in our recent study.¹⁹ Analysis performed by means of high-resolution x-ray diffraction shows that the GaAsBi/GaAs layers are coherent with the GaAs substrates and are compressively strained. Significantly reduced diffuse scattering indicates that the QW interfaces are of a very high quality, i.e., low roughness. Using x-ray rocking curve simulations,^{16,19} we determined the Bi content, x , and QW width, d_{QW} , for sample #1 to be $x = 3.5\%$, $d_{QW} = 13.0$ nm; for sample #2 to be $x = 4.1\%$, $d_{QW} = 7.5$ nm; and for sample #3 to be $x = 6.0\%$, $d_{QW} = 11$ nm, i.e., the Bi concentration in these samples covers the range from 3.5% to 6%. It has been recently shown that the electronic structure of GaAs_{1-x}Bi_x changes significantly in this range.¹⁸ The exciton reduced mass anomalously increases with x below 5%, whereas it decreases and follows a conventional behavior for $x > 5\%$.

^{a)}Electronic address: ymazur@uark.edu.

Moreover, far infrared absorption measurements have demonstrated the existence of acceptor states related to Bi only within the concentration region of the anomalous behavior.¹² Therefore, the samples chosen for investigation are of particular interest for PL measurements.

The PL measurements were performed in a variable temperature, 10–300 K, closed-cycle helium cryostat using the 532 nm line from a doubled Nd:YAG laser for excitation. The laser spot diameter was $\sim 20 \mu\text{m}$ with power in the range of $\sim (10^{-6} - 10^2)$ mW. The PL signal was dispersed by a 0.5-m single-grating monochromator and detected by a LN-cooled OMAV: InGaAs photodiode detector array.

Figure 1 shows the PL spectra of the GaAsBi QW samples measured at low temperature, $T = 15 \text{ K}$, and moderate excitation intensity allowing distinct observation of differences in the PL line-shape. The energy position of the PL maximum, E_{max} , and full width at half maximum (FWHM), Γ , of the PL bands are found to be: $E_{max} = 1.182 \text{ eV}$ and $\Gamma = 74 \text{ meV}$ for sample #1; $E_{max} = 1.241 \text{ eV}$ and $\Gamma = 68 \text{ meV}$ for sample #2; and $E_{max} = 1.085 \text{ eV}$ and $\Gamma = 33 \text{ meV}$ for sample #3. The spectra are normalized with respect to their maxima. Following arguments of Refs. 16 and 19, we assign each PL band shown in Fig. 1 to the exciton ground state emission in the corresponding QW. As one can see, all the bands are strongly asymmetric towards lower energy. This asymmetry serves as a measure of disorder in the bismide QW structure caused by fluctuating concentration and clustering of Bi or by the localized states related to Bi incorporation.^{2,17} At low temperatures and excitation intensities, the excitons are at most trapped by defects, and the excitonic PL line shape reflects the distribution of states in defect structures. Hence, the larger PL line asymmetry seen in Fig. 1 for samples #1 and #2 as compared to that observed in the sample #3 indicates a stronger disorder in these samples. In order to investigate the effect of this disorder on the exciton processes in $\text{GaAs}_{1-x}\text{Bi}_x$ QWs, we measure the PL spectra under different excitation intensities.

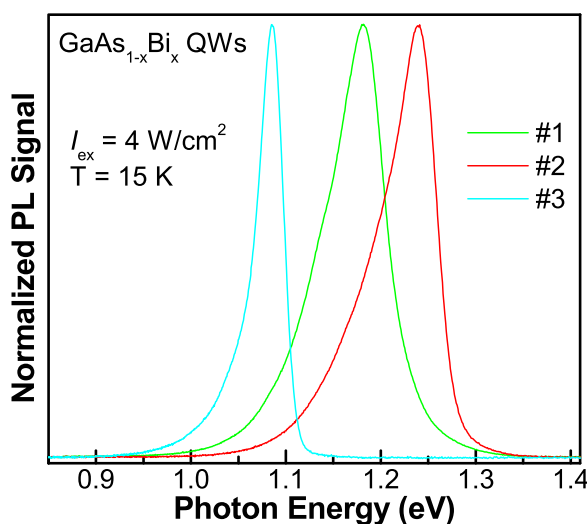


FIG. 1. Low temperature ($T = 15 \text{ K}$) PL spectra measured at $I_{ex} = 4 \text{ W/cm}^2$ in $\text{GaAs}_{1-x}\text{Bi}_x$ QWs with $x = 3.5\%$ (sample #1), $x = 4.1\%$ (sample #2), and $x = 6.0\%$ (sample #3). Spectra are normalized to the PL maxima for comparison.

Figure 2 shows the results of these measurements for sample #1 (Fig. 2(a)), sample #2 (Fig. 2(b)), and sample #3 (Fig. 2(c)) for excitation intensities varied by eight orders of magnitude. A common feature in all spectra is a pronounced blue-shift by ~ 40 to $\sim 80 \text{ meV}$ upon changing I_{ex} from 10^{-4} W/cm^2 to 10^4 W/cm^2 . The asymmetry of the line shape also changes between low and high power excitations. The origins of these observed low- and high-energy asymmetries differ from each other in our QW samples. In order to understand this difference, let us consider the dependence of the spectrally integrated PL on the excitation intensity, Fig. 3. One can see here that the excitation-dependent PL spectra behave differently in the low- and high-intensity regions. In each of these regions, the experimental data can be fit by straight lines given by the equation, $I_{PL} = AI_{ex}^\zeta$, which is characterized by the slope, ζ . For the low-intensity region, $2.4 \times 10^{-4} - 0.1 \text{ W/cm}^2$, the PL intensity increases nearly linearly with excitation ($\zeta \approx 1$) in all samples. This linear dependence is typical for localized excitons. Further increase of the excitation power density results in a sublinear dependence, $\zeta = 0.748, 0.739,$ and 0.884 for samples #1, #2, and #3, respectively. The observed dependence of the PL intensity on the excitation power density can be explained by a competition of the exciton recombination through radiative and nonradiative channels and by carrier localization. At low temperatures and low excitations, the excitons tend to be localized and cannot reach nonradiative recombination centers. Therefore, under a moderate pumping, the excitons occupy the localized states and recombine predominantly

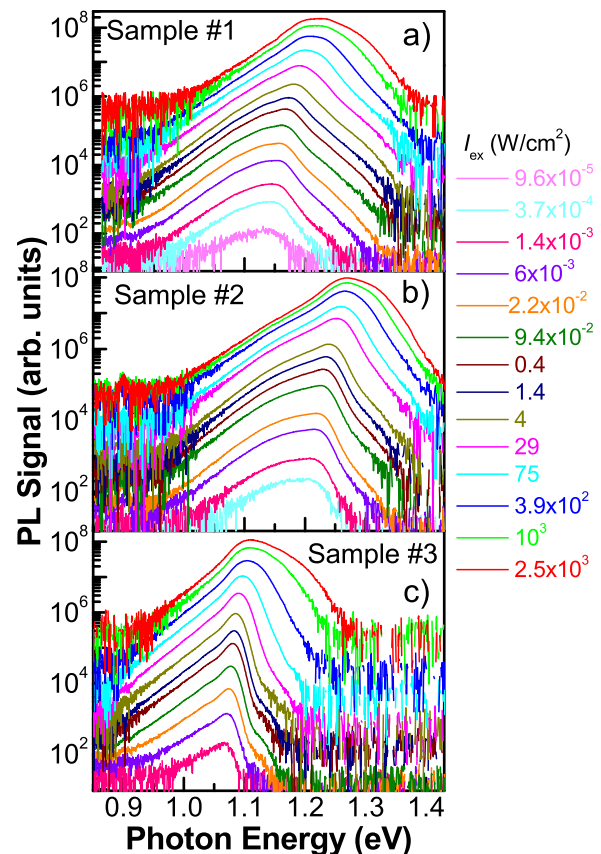


FIG. 2. PL spectra measured at various excitation intensities and temperature, $T = 15 \text{ K}$, of sample #1 (a), sample #2 (b), and sample #3 (c).

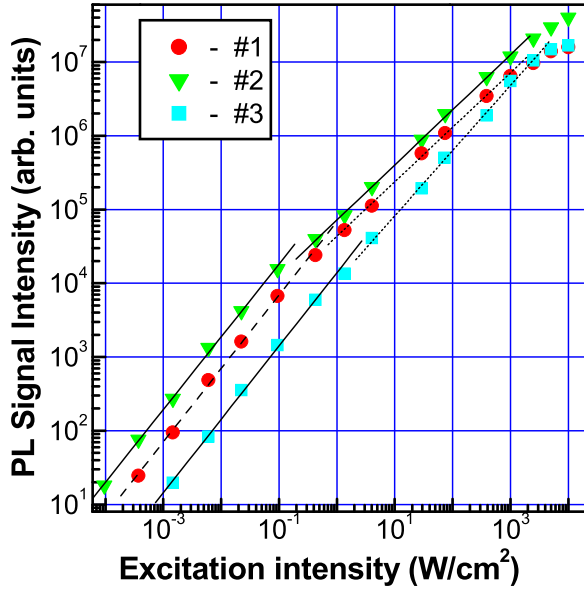


FIG. 3. Integrated PL intensity of sample #1, sample #2, and sample #3 measured at $T = 15$ K with different excitation intensities. Lines show fits to $I_{PL} = AI_{ex}^{\zeta}$ for separate excitation regimes.

radiatively. As a result, the integrated PL intensity remains a linear function of the excitation power density through this range. Increase of the excitation intensity further favors filling the localized states which are limited in number. This then allows for a considerable portion of the excitons to become free and subsequently, easily reach nonradiative recombination centers and recombine nonradiatively. While an increase of excitation intensity makes the free excitons dominant, their nonradiative recombination already determines the dynamics of the whole non-equilibrium system of excitons. Nonradiative recombination reduces the number of excitons which can recombine radiatively. As a result, the PL intensity becomes weaker at the same level of excitation and its dependence on I_{ex} becomes sublinear. Thus, the change of the $I_{PL} = AI_{ex}^{\zeta}$ dependence seen in Fig. 3 is caused by exciton localization at the low temperature and low excitation power densities and by a nonradiative decay of excitons at high I_{ex} values. Since ζ is smaller in samples #1 and #2 than in sample #3, we conclude that the nonradiative losses of free excitons are smaller in sample #3. The origins of exciton localization in bismuth QWs include fluctuations in bismuth content, non-random bismuth distributions, interface inhomogeneities, etc.^{11,17} Free excitons can be efficiently trapped by these defects at low temperatures. If temperature increases up to room temperature, the character of the $I_{PL} = AI_{ex}^{\zeta}$ dependence has to change substantially. At this temperature limit, the excitons are predominantly free due to a thermal activation and coexist with free electron-hole pairs in a QW. Therefore, the nonradiative recombination dominates even at the lowest excitation intensities that we observed experimentally.

The contributions of localized and free excitons determine the PL line shape as a function of temperature and excitation intensity. In order to evaluate these contributions, we consider a simple model within the framework of rate equations. Let us introduce coupled free and localized exciton

systems. The free exciton system is characterized by an energy, E_1 , decay rate, $\tau_{d1}^{-1} = \tau_{r1}^{-1} + \tau_{nr1}^{-1}$, where τ_{r1} and τ_{nr1} are the times of radiative and nonradiative exciton recombination, respectively, and a population number, n_1 . The localized exciton system has energy, E_i , decay rate, $\tau_{di}^{-1} = \tau_{ri}^{-1} + \tau_{nri}^{-1}$, with τ_{ri} and τ_{nri} being the times of radiative and nonradiative localized exciton recombination, respectively, and a population number, n_i , for the impurity site i with the finite density of states N_i . A free exciton can be trapped by an impurity site i with the rate τ_c^{-1} , thus transforming to a localized exciton. Similarly, a trapped exciton can be thermally released, becoming free with energy, E_1 , at a rate of τ_{th}^{-1} . Thus, the rate equations for these coupled systems can be written as follows:

$$\begin{aligned} \frac{dn_1}{dt} &= \sigma I_{ex} - \frac{n_1}{\tau_{d1}} - \frac{n_1(N_i - n_i)}{\tau_c N_i} + \frac{n_i}{\tau_{th}}, \\ \frac{dn_i}{dt} &= -\frac{n_i}{\tau_{di}} - \frac{n_i}{\tau_{th}} + \frac{n_1(N_i - n_i)}{\tau_c N_i}. \end{aligned} \quad (1)$$

Here, σI_{ex} is an exciton generation rate and σ is a scaling parameter for I_{ex} . In a steady state regime, $dn_1/dt = 0$, $dn_i/dt = 0$, and thus the explicit solution of Eq. (1) takes the form

$$\begin{aligned} n_1 &= [\sigma I_{ex} - n_i/\tau_{di}] \tau_{d1}, \\ n_i &= \left[B(I_{ex}) - \sqrt{(B(I_{ex}))^2 - 4\sigma I_{ex} \tau_{di} N_i} \right] / 2, \end{aligned} \quad (2)$$

with $B(I_{ex}) = N_i + \sigma I_{ex} + N_i \tau_c (\tau_{th} + \tau_{di}) / (\tau_{d1} \tau_{th})$. Taking into account that the PL intensity is described in terms of population numbers, one has $I_{PL}^1 = C n_1 / \tau_{r1}$ and $I_{PL}^i = C n_i / \tau_{ri}$ for the free and localized exciton emissions, respectively. C is a factor which depends on the actual experimental arrangement but is (essentially) identical for free and localized excitons. Finally, the expression

$$I_{PL} = I_{PL}^1 + I_{PL}^i \quad (3)$$

gives the total PL intensity and can be used for analysis of the experimental data. As seen in Fig. 2, for low to moderate I_{ex} the shape of the PL bands related to free and bound excitons does not change significantly with I_{ex} . For this reason, we assume that the net change of the PL spectra of the QW structure is determined mainly by the ratio of contributions from free and localized (bound) excitons. This ratio is determined principally by Eq. (2). It is seen from Eq. (2) that if $I_{ex} \rightarrow \infty$, $n_i \rightarrow N_i$, i.e., the contribution of the localized excitons saturates. Thus, under high excitation power density, the behavior of the exciton system is determined exclusively by free excitons and presumably by the electron-hole pairs arising due to dissociation of free excitons. In case of low excitation intensity and temperature, the dynamics of the exciton system is determined by a competition between free and localized excitons, which in turn is governed by relaxation and coupling parameters in Eq. (2).

The energy of the low temperature ($T = 15$ K) PL maximum, $E_{\max}(I_{ex})$, and the FWHM, $\Gamma(I_{ex})$, are shown in Figs. 4(a), 4(b), and 4(c), for samples #1, #2, and #3, respectively.

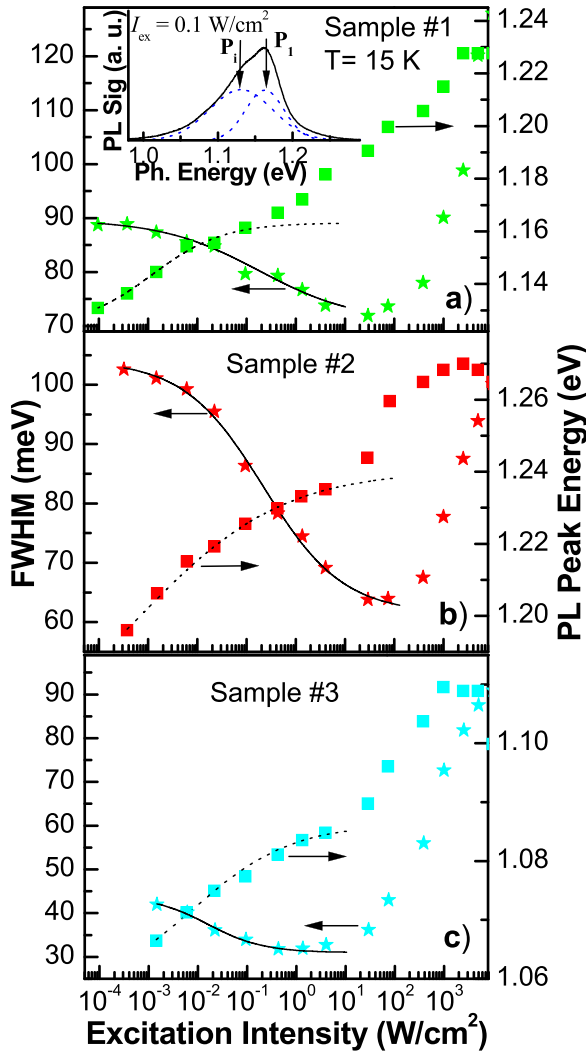


FIG. 4. PL peak energy and FWHM as the functions of excitation intensity, I_{ex} , measured at low temperature ($T = 15$ K) from sample #1 (a), sample #2 (b), and sample #3 (c). Lines show the theoretical dependences calculated using Eqs. (2) and (3). Inset: decomposition of the low temperature, low excitation intensity PL spectrum of sample #1 by two Gaussians.

Common to all samples with increasing I_{ex} up to ~ 1 W/cm² is the increase of $E_{\max}(I_{ex})$ and the decrease of $\Gamma(I_{ex})$. Then, $E_{\max}(I_{ex})$ reaches a plateau for all samples at a similar I_{ex} . However, $\Gamma(I_{ex})$ reaches a minimum at significantly different excitation intensities for each sample which corresponds to a further increase in $E_{\max}(I_{ex})$. This behavior of $E_{\max}(I_{ex})$ and $\Gamma(I_{ex})$ can be understood within the framework of our free and localized exciton model. In order to apply Eqs. (2) and (3) to describe the data in Fig. 4, we model the spectral distribution of both the free and localized exciton systems as Gaussians, $I = A \exp\{-(E - E_0)^2/2\omega^2\}$, with $\text{FWHM} = 2\sqrt{2 \ln 2} \omega$. The result of deconvolving the PL in sample #1 for low excitation intensity is shown in the inset of Fig. 4(a) with $E_{\max}^i = 1.131$ eV, $\Gamma^i = 83$ meV for the localized exciton band P_i , and $E_{\max}^1 = 1.163$ eV, $\Gamma^1 = 50$ meV for the free exciton band P_1 . A similar procedure is carried out for all PL spectra. Now, since the data in Fig. 4 were measured at low temperature ($T = 15$ K), we set $\tau_{th} \rightarrow \infty$ in Eq. (1), thus neglecting the thermal activation of localized excitons. Then, using our previous data for free and localized exciton

decay times in quantum well-quantum dot structures,^{20–23} we put $\tau_{d1} = 600$ ps and $\tau_{d2} = 1.5$ ns in Eq. (2). As a result, we are left only two fitting parameters: τ_c^{-1} defining the rate of free exciton trapping by defects, and N_i determining the density of defect sites which can be occupied by localized excitons. This latter parameter governs the saturation in the localized exciton system. Fig. 4 shows the results of these fits carried out using Eqs. (2) and (3) in the low excitation intensity region for all samples. The $E_{\max}(I_{ex})$ and $\Gamma(I_{ex})$ dependences were derived from Eq. (3). The quality of the fit demonstrates the adequacy of the model to the real situation in the dilute bismuthide GaAs_{1-x}Bi_x QW structures under investigation. We found that $\tau_c = 23$ ps in sample #1, $\tau_c = 14$ ps in sample #2, and $\tau_c = 57$ ps in sample #3. For N_i , we determined a ratio $N_1^1 : N_2^2 : N_3^3 = 1:1.8:0.3$ for samples #1, #2, #3, respectively. Thus, sample #3 possesses the highest structural quality that is immediately reflected in its low temperature PL FWHM value (see Fig. 1).

Following the results of the above analysis, the behavior of $E_{\max}(I_{ex})$ and $\Gamma(I_{ex})$, and hence the PL line shape in the low excitation intensity regime is determined by the relative contributions of the localized and free excitons. In this regime, these contributions are comparable and the PL maximum is modified by the low energy PL band of the localized excitons. The FWHM is accordingly broad as a result of an overlap of two neighboring PL bands. Increasing I_{ex} saturates the localized band allowing the free exciton band to increase alone. This shifts the apparent $E_{\max}(I_{ex})$ toward the higher energy free exciton PL band, while the FWHM tends toward the smaller free exciton band value, which is clearly demonstrated in Fig. 4. Further blue shift of $E_{\max}(I_{ex})$ and the increase of $\Gamma(I_{ex})$ with I_{ex} are mainly related to the behavior of free excitons in the QW resulting from band state filling and the emergence of QW excited states. For a full description of $E_{\max}(I_{ex})$ and $\Gamma(I_{ex})$ in the case of strong optical excitation, one has to take into account exciton dissociation, coexistence of excitons and free electron-hole pairs, many-body effects, and band gap renormalization. All these effects are, however, beyond the scope of this study.

Nevertheless, let us consider a property of free excitons related to composition in the GaAs_{1-x}Bi_x QWs.¹² Indeed, following far-infrared absorption results from Ref. 12, the exciton reduced mass in samples #1 and #2 has to be larger than that in the sample #3. For observation of an effect of abnormal variation of reduced mass with the Bi concentration, we increased the temperature and consequently the excitation intensity in order to release excitons from the traps, Fig. 5. Thus, a predominantly free exciton system in the QW was prepared. In order to see distinctly a change of the PL line shape, all spectra are normalized and plotted with the same center position. The PL band in sample #2 remains significantly wider in comparison with that of sample #3 even at this high temperature where the contribution of crystal inhomogeneity is less pronounced and the line shape is defined mainly by the free exciton energy distribution. We consider an excess broadening of the PL band in sample #2 to be a result of higher reduced exciton mass in this dilute bismuthide. Indeed, broadening may be partly attributed to

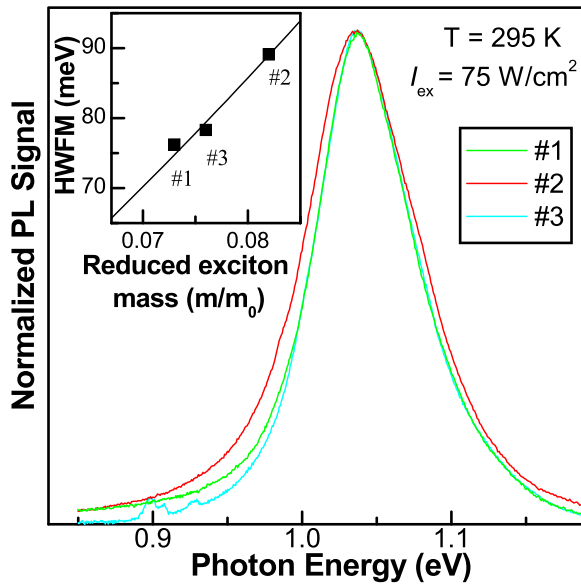


FIG. 5. High temperature ($T=295$ K) PL spectra measured at $I_{ex}=75$ W/cm² for all samples. Spectra are normalized to the PL maxima and reduced to the position of the PL band in sample #3 for comparison. Inset: Dependence of the FWHM value on the reduced exciton mass in samples #1, #2, and #3. Solid line shows the $\Gamma = \kappa\mu^{3/2}$ function.

compositional disorder. Excitons in different spatial regions of the QW have different optical transition energies resulting in an inhomogeneous broadening of the transition energy. In semiconductor alloys,²⁴ this broadening can be related to the reduced excitonic mass, μ , assuming the excitonic line shape is Gaussian. In this case, Γ can be shown to vary as, $\Gamma \propto \mu^{3/2}$.^{24,25} Fig. 5, inset shows this relationship, solid line, with the experimental points from this study. Here, the Γ values are taken from our data and the reduced masses are determined from Ref. 12 for Bi compositions close to that in our samples. The exciton PL band in our samples differs from purely Gaussian and therefore the relation between Γ and μ can be used only for a qualitative estimation. Nevertheless, we find a good agreement to the theory here indicating that the free exciton mass influences the FWHM that we observe experimentally in Fig. 5.

III. CONCLUSIONS

Summarizing we have studied a set of high quality single quantum well samples of GaAs_{1-x}Bi_x semiconductor alloys with bismuth concentration not exceeding 6% and well width ranging from 7.5 to 13 nm. These samples were grown by molecular beam epitaxy on a GaAs substrate at low temperature and characterized by means of high-resolution x-ray diffraction in order to establish the true Bi concentration and structural quality of the QWs. Strongly non monotonous PL band dependence on the excitation intensity is revealed and interpreted in terms of optically unresolved contributions from saturable emission of localized excitons and free exciton emission.

ACKNOWLEDGMENTS

The authors acknowledge the financial support by the US National Science Foundation (NSF) via Grant No. DMR-0520550 and MWN (Material World Network) Program between the NSF (Grant No. DMR-1008107) and the Deutsche Forschungsgemeinschaft (Grant No. Li 580/8-1). S.-Q. Yu acknowledges support by NSF Career Award No. DMR-1149605.

¹S. Tixier, M. Adamczyk, T. Tiedje, S. Francoeur, A. Mascarenhas, P. Wei, and F. Schiettekatte, *Appl. Phys. Lett.* **82**, 2245 (2003).

²T. Tiedje, E. C. Young, and A. Mascarenhas, *Int. J. Nanotechnol.* **5**, 963 (2008).

³X. Lu, D. A. Beaton, R. B. Lewis, T. Tiedje, and Y. Zhang, *Appl. Phys. Lett.* **95**, 041903 (2009).

⁴Y. Tominaga, Y. Kinoshita, K. Oe, and M. Yoshimoto, *Appl. Phys. Lett.* **93**, 131915 (2008).

⁵K. Bertulis, A. Krotkus, G. Aleksejenko, V. Pacebutas, R. Andromavicius, and G. Molis, *Appl. Phys. Lett.* **88**, 201112 (2006).

⁶K. Alberi, J. Wu, W. Walukiewicz, K. M. Yu, O. D. Dubon, S. P. Watkins, C. X. Wang, X. Liu, Y.-J. Cho, and J. Furdyna, *Phys. Rev. B* **75**, 045203 (2007).

⁷G. Ciatto, E. C. Young, F. Glas, J. Chen, R. Alonso Mori, and T. Tiedje, *Phys. Rev. B* **78**, 035325 (2008).

⁸Y. Tominaga, K. Oe, and M. Yoshimoto, *Appl. Phys. Express* **3**, 062201 (2010).

⁹G. Ciatto, M. Thomasset, F. Glas, X. Lu, and T. Tiedje, *Phys. Rev. B* **82**, 201304(R) (2010).

¹⁰G. Ciatto, P. Alippi, A. A. Bonapasta, and T. Tiedje, *Appl. Phys. Lett.* **99**, 141912 (2011).

¹¹A. G. Norman, R. France, and A. J. Ptak, *J. Vac. Sci. Technol. B* **29**, 03C121 (2011).

¹²G. Pettinari, H. Engelkamp, P. C. M. Christianen, J. C. Maan, A. Polimeni, M. Capizzi, X. Lu, and T. Tiedje, *Phys. Rev. B* **83**, 201201(R) (2011).

¹³C. A. Broderick, M. Usman, S. J. Sweeney, and E. P. O'Reilly, *Semicond. Sci. Technol.* **27**, 094011 (2012).

¹⁴Z. Batool, K. Hild, T. J. C. Hosea, X. Lu, T. Tiedje, and S. J. Sweeney, *J. Appl. Phys.* **111**, 113108 (2012).

¹⁵G. Pettinari, A. Patanè, A. Polimeni, M. Capizzi, X. Lu, and T. Tiedje, *Appl. Phys. Lett.* **100**, 092109 (2012).

¹⁶Yu. I. Mazur, V. G. Dorogan, M. Schmidbauer, G. G. Tarasov, S. R. Johnson, X. Lu, S.-Q. Yu, Zh. M. Wang, T. Tiedje, and G. J. Salamo, *Nanotechnology* **22**, 375703 (2011).

¹⁷S. Imhof, A. Thränhardt, A. Chernikov, M. Koch, N. S. Köster, K. Kolata, S. Chatterjee, S. W. Koch, X. Lu, S. R. Johnson, D. A. Beaton, T. Tiedje, and O. Rubel, *Appl. Phys. Lett.* **96**, 131115 (2010).

¹⁸G. Pettinari, A. Polimeni, J. H. Blokland, R. Trotta, P. C. M. Christianen, M. Capizzi, J. C. Maan, X. Lu, E. C. Young, and T. Tiedje, *Phys. Rev. B* **81**, 235211 (2010).

¹⁹Yu. I. Mazur, V. G. Dorogan, M. Benamara, M. E. Ware, M. Schmidbauer, G. G. Tarasov, S. R. Johnson, X. Lu, S.-Q. Yu, T. Tiedje, and G. J. Salamo, *J. Phys. D: Appl. Phys.* **46**, 065306 (2013).

²⁰Yu. I. Mazur, V. G. Dorogan, E. Marea, Jr., P. M. Lytvyn, Z. Ya. Zhuchenko, G. G. Tarasov, and G. J. Salamo, *New J. Phys.* **11**, 043022 (2009).

²¹Yu. I. Mazur, V. G. Dorogan, D. Guzun, E. Marega, Jr., G. J. Salamo, G. G. Tarasov, A. O. Govorov, P. Vasa, and C. Lienau, *Phys. Rev. B* **82**, 155413 (2010).

²²Yu. I. Mazur, V. G. Dorogan, E. Marega, Jr., Z. Ya. Zhuchenko, M. E. Ware, M. Benamara, G. G. Tarasov, P. Vasa, C. Lienau, and G. J. Salamo, *J. Appl. Phys.* **108**, 074316 (2010).

²³Yu. I. Mazur, V. G. Dorogan, E. Marega, M. Benamara, Z. Ya. Zhuchenko, G. G. Tarasov, C. Lienau, and G. J. Salamo, *Appl. Phys. Lett.* **98**, 083118 (2011).

²⁴E. D. Jones, A. A. Allerman, S. R. Kurtz, N. A. Modine, and K. K. Bajaj, *Phys. Rev. B* **62**, 7144 (2000).

²⁵M. Muñoz, F. H. Pollak, M. Kahn, D. Ritter, L. Kronik, and G. M. Cohen, *Phys. Rev. B* **63**, 233302 (2001).